Role of Mg^{2+} in Modifying the Environment of Radiolytically Produced Silver Atoms in A Zeolites: Electron Spin Resonance and Electron Spin Echo Modulation Spectroscopy Studies

M. Narayana and Larry Kevan*

Contribution from the Department of Chemistry, University of Houston, Houston, Texas 77004.
Received March 4, 1985

Abstract: Radiolytically generated silver atoms have been studied in A zeolites by electron spin resonance (ESR) and electron spin echo modulation (ESEM) spectroscopy. A thermally unstable Ag^0 species of low abundance, $Ag^0(C)$, reported earlier by us (*J. Chem. Phys.* **1982**, *76*, 3999) increases in intensity as sodium ions in the A zeolite are progressively replaced by Mg^{2+} and becomes the major Ag^0 species in Na_2Mg_5A zeolite. In zeolites with Na > eight and Mg < two ions per unit cell, decay of $Ag^0(C)$ on warming of the sample above 100 K results in enhancement of the major silver atom species observed in all other monovalent ion A zeolites, $Ag^0(A)$. Analysis of ESEM data of $Ag^0(C)$ in Na_2Mg_5A zeolite prepared with deuterated water and exchanged with the ^{109}Ag isotope indicates that $Ag^0(C)$ interacts with four deuterons at 0.33 nm with an isotropic hyperfine coupling of 0.1 MHz and four more deuterons at 0.36 nm. The possible locations and decay pathways of $Ag^0(C)$ in the A zeolite structure are discussed.

The ion exchange of Ag^+ is known to markedly affect the stability and catalytic properties of zeolites in specific reactions[1-3] like the oxidation of ethylene. The redox behavior of Ag-exchanged zeolites has been investigated chemically by several authors.[4-8] The ability of silver-loaded zeolites to photochemically cleave water into H_2 and O_2 has been observed[9-11] but not fully understood. It has been proposed that monomeric or small clusters of silver atoms, reoxidizable to monomeric Ag^+, are active photochemical intermediates. In this context, it is important to know the location and immediate environment of these silver atoms.

Isolated and small clusters of silver atoms are paramagnetic and thus amenable to characterization by electron spin resonance (ESR) techniques. Because of the s character of the unpaired electron, an isolated silver atom exhibits a large hyperfine coupling to its own nucleus which is quite sensitive to the immediate environment.[12-14] Several ESR studies of silver atoms generated by γ-radiolysis of silver-loaded zeolites at 77 K have been reported.[15-17] Electron spin echo modulation (ESEM) spectroscopy is a powerful complementary technique to ESR and can be used to measure the weak hyperfine and quadrupolar interactions[18,19] between paramagnetic probes and surrounding magnetic nuclei, which are not typically resolvable by conventional ESR methods.

Using ESEM methods we have recently been able to characterize[20] different Ag^0 species observed in A, X, and Y zeolites on γ-irradiation at 77 K. In that study a thermally unstable Ag^0 species of low abundance, $Ag^0(C)$, was observed in Li^+- and Ca^{2+}-exchanged A zeolites. In this paper, we demonstrate how to enhance the yield of this species by ion exchange of the A zeolite with Mg^{2+}. Unlike the dominant Ag^0 species seen in most A zeolites, silica, and alumina, $Ag^0(A)$, the $Ag^0(C)$ species observed in magnesium-exchanged A zeolites interacts with four water molecules and is stable only below 100 K. Above 100 K, in the sodium-rich A zeolites, $Ag^0(C)$ is converted to the dominant Ag^0 species, $Ag^0(A)$, which interacts with only two water molecules. In magnesium-rich A zeolites $Ag^0(C)$ decays either into a diamagnetic cluster or back to Ag^+.

Experimental Section

Linde 4A zeolite, washed with a 0.1 M solution of sodium acetate, was ion exchanged with 0.1 M solutions of magnesium acetate at 333 K for several days to obtain Na_2Mg_5A zeolite, where the numbers refer to the primitive unit cell of A zeolite. The final sodium and magnesium contents were obtained by commercial atomic absorption analysis. Thermogravimetric experiments indicated the number of water molecules per primitive cell to be about 40, which agrees very well with the preparation of Dyer and Enamy.[21] Several other A zeolite samples with differing Mg^{2+} concentration were also prepared such as $Na_{11.8}Mg_{0.1}A$, $Na_{10}Mg_8A$, and Na_8Mg_2A. In these zeolites, the magnesium concentration was estimated by assuming complete exchange. Attempts to obtain a fully magnesium-exchanged A zeolite, Mg_6A, were not successful.[21,22] Silver ions were then ion exchanged into these various magnesium A zeolites by ion exchange with 1 mM silver acetate solutions at room temperature to the extent of 0.7 Ag^+ per primitive cell. Isotopically enriched ^{109}Ag (Oak Ridge National Labs) was used in some samples. The samples were deuterated either by soaking in D_2O (Aldrich, Gold Label) in a vacuum desiccator or by dehydrating the sample on a vacuum line at 623 K, oxidizing in 500 torr of O_2 for 3 h at the same temperature, again evacuating it to a residual pressure of 2×10^{-6} torr, and then exposing the sample to D_2O vapor at ambient temperature for 6 h. The samples were then sealed in 3-mm o.d. Suprasil quartz tubes

(1) Breck, D. W.; Milton, R. M. U. S. Patent 3013985, 1958.
(2) Giordane, N.; Bart, J. c. J.; Maggiore, R. *Z. Phys. Chem.* **1981**, *124*, 97.
(3) Nitta, M.; Tanabe, K.; Hattori, H. *Bull. Jpn. Pet. Inst.* **1972**, *15*, 113.
(4) Riekert, L. *Ber. Bunsenges. Phys. Chem.* **1969**, *73*, 331.
(5) Tsutsumi, K.; Takahashi, H. *Bull. Chem. Soc. Jpn.* **1972**, *45*, 2332.
(6) (a) Beyer, H. K.; Jacobs, P. A.; Uytterhoeven, J. B. *J. Chem. Soc., Faraday Trans. 1* **1976**, *72*, 674. (b) Jacobs, P. A.; Uytterhoeven, J. B.; Beyer, H. K. *Ibid.* **1979**, *75*, 56.
(7) Texter, J.; Gonsiorowski, T.; Kellerman, R. *Phys. Rev. B* **1981**, *23*, 4407.
(8) Gellens, L. R.; Mortier, W. J.; Uytterhoeven, J. B. *Zeolites* **1981**, *1*, 11.
(9) Leutwyler, S.; Schumacher, E. *Chimia* **1977**, *31*, 475.
(10) (a) Jacobs, P. A.; Uytterhoeven, J. B.; Beyer, H. K. *J. Chem. Soc., Chem. Commun.* **1977**, *128*. (b) Kuznicki, S.; Eyring, E. M. *J. Am. Chem. Soc.* **1978**, *100*, 6790.
(11) (a) Sulzberger, B.; Calzaferri, G. *J. Photochem.* **1982**, *19*, 321. (b) Calzaferri, G.; Hug, S.; Hugentobler, T.; Sulzberger, B. *Ibid.* **1984**, *26*, 109.
(12) Bales. B. L.; Kevan, L. *J. Chem. Phys.* **1971**, *55*, 1327.
(13) Kevan, L.; Hase, H.; Kawabata, K. *J. Chem. Phys.* **1977**, *66*, 3834.
(14) (a) Narayana, P. A.; Becker, D.; Kevan, L. *J. Chem. Phys.* **1978**, *68*, 652. (b) Ichikawa, T.; Kevan, L.; Narayana, P. A. *Ibid.* **1979**, *71*, 3792.
(15) Abou-Kais, A.; Vedrine, J. C.; Naccache, C. *J. Chem. Soc., Faraday Trans. 1* **1978**, *74*, 959.
(16) Zhitnikov, R. A.; Peregud, D. P. *Sov. Phys.-Solid State (Engl. Transl.)* **1980**, *22*, 1141.
(17) (a) Popovich, G. M.; Shekhobalova, V. I.; Malkin, A. I. *Zh. Fiz. Khim.* **1983**, *57*, 2194. (b) Popovich, G. M.; Shekhobalova, V. I.; Malkin, A. I. *Ibid.* **1983**, *57*, 2199.
(18) (a) Mims, W. B.; Peisach, J.; Davis, J. L. *J. Chem. Phys.* **1977**, *66*, 5536. (b) Mims, W. B.; Peisach, J. In "Biological Applications of Magnetic Resonance"; Schulman, R. G., Ed.; Academic Press: New York, 1979; p 221.
(19) Kevan, L. In "Time Domain Electron Spin Resonance"; Kevan, L., Schwartz, R. N., Eds.; Wiley-Interscience: New York, 1979; Chapter 8.
(20) Narayana, M.; Kevan, L. *J. Chem. Phys.* **1982**, *76*, 3999.
(21) Dyer, A.; Enamy, H. *Zeolites* **1981**, *1*, 7.
(22) Wolf, F.; Pilchowski, K.; Danes, F.; Ceacareanu, D.; *Wiss. Z. Univ. Halle* **1972**, *21*, 87.

0002-7863/85/1507-4643$01.50/0

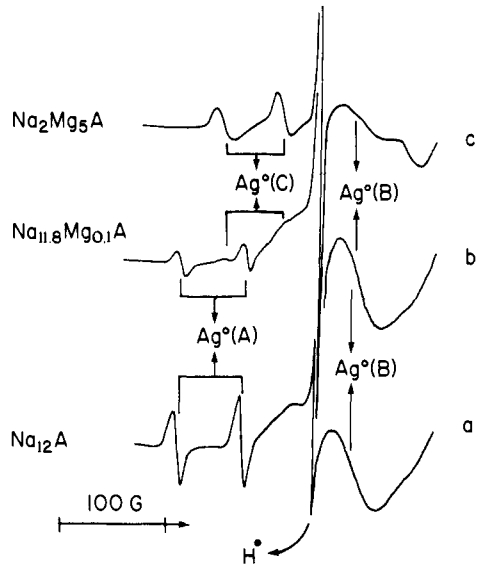

Figure 1. ESR spectra at 77 K of Ag^0 in A zeolites with different concentrations of Mg^{2+} with only the low-field part of the spectra being shown: (a) in fully sodium-exchanged $Na_{12}A$ zeolite $Ag^0(A)$ is seen as the dominant silver species; (b) exchange of 0.1 Mg^{2+} per unit cell is sufficient for the weak but distinct appearance of $Ag^0(C)$; and (c) when Mg^{2+} is present at five ions per unit cell, Ag(C) is the dominant species and $Ag^0(A)$ is not seen. The sharp singlet is the low-field resonance of a hydrogen atom, also produced by γ-irradiation.

and γ-irradiated at 77 K in a ^{60}Co γ-source to a dose of 1 Mrad.

ESR spectra were recorded at 77 K with a modified Varian E-4 spectrometer, and the ESEM spectra were recorded at 4.2 K with a home-built spectrometer.[23]

Results

The ESR spectrum of isolated Ag^0, obtained by electron capture by Ag^+ on γ-irradiation, consists of two doublets of equal intensity due to the two almost equally abundant isotopes (^{107}Ag, ^{109}Ag, $I = {}^1/_2$). Our earlier results[20] on Ag^0 in A zeolites can be summarized as follows. In all the monovalent ion exchanged A zeolites and in Ca_4Na_4A two major Ag^0 species, $Ag^0(A)$ and $Ag^0(B)$, were observed. $Ag^0(A)$ cannot be formed in faujasite type (X or Y) zeolites or in zeolites of higher silica content such as mordenite or ZSM5. ESEM analysis indicated that $Ag^0(A)$ is coordinated to two waters and is located inside the small β-cages of the zeolite lattice. $Ag^0(A)$ is stable to brief warming to $\sim$130 K above which it rapidly decays to form Ag_y^{x+} ($x < y < 5$) clusters. $Ag^0(B)$ has a smaller hyperfine coupling, 1480 vs. 1980 MHz for $Ag^0(A)$, decays rapidly on warming of the samples above $\sim$110 K, and results in an increase of $Ag^0(A)$. Because of the shorter electron spin echo phase memory times, the ESEM data from $Ag^0(B)$ could not be quantitatively analyzed, but the stronger ^{27}Al modulation compared with that observed for $Ag^0(A)$ indicates that $Ag^0(B)$ is likely to be at the center of the six ring windows between the large α- and small β-cages of the A zeolite.[24] In two of the A zeolites, $Li_{12}A$ and Ca_6A, a third Ag^0 species, $Ag^0(C)$ with a hyperfine coupling of 1778 MHz, intermediate between those of $Ag^0(A)$ and $Ag^0(B)$, was observed. It has much lower intensity and decayed very rapidly, often during the few seconds of sample transfer from the irradiation dewar to the ESR dewar.

The ESR spectra of Ag^0 in A zeolites with different Mg^{2+} concentrations are shown in Figures 1 and 2. Only the low-field parts of the spectra are shown to reduce the complexity. The sharp resonances due to hydrogen atoms, also formed during the radiolysis, are used as field markers. In Figure 1 it is clearly seen that even a very small concentration of Mg^{2+} in the zeolite induces the formation of $Ag^0(C)$, and in Na_2Mg_5A $Ag^0(A)$ is no longer

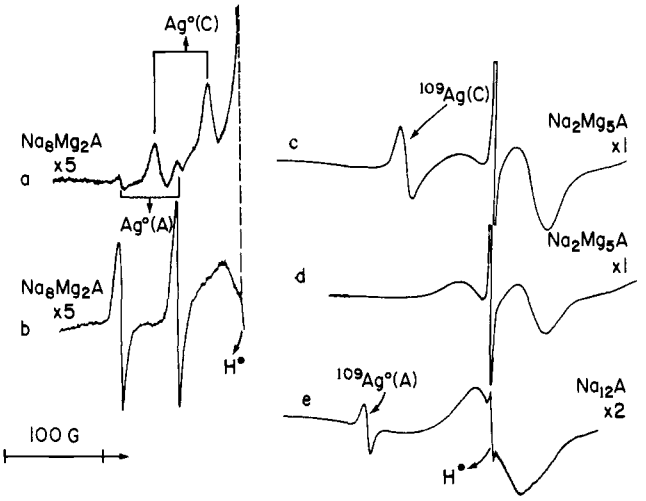

Figure 2. ESR spectra at 77 K of Ag^0 in A zeolites with different concentrations of Mg^{2+}: (a) $Ag^0(C)$ as well as $Ag^0(A)$ is seen in Na_8Mg_2A immediately after γ-irradiation at 77 K; (b) on warming this sample to $\sim$100 K for 3–5 s $Ag^0(C)$ disappears and $Ag^0(A)$ grows in intensity; (c) Na_2Mg_5A zeolite, exchanged with $^{109}Ag^+$, shows only the $Ag^0(C)$ species; (d) on warming the sample in (c) to 100 K for 3–5 s, $Ag^0(C)$ disappears but $Ag^0(A)$ *does not* form; (e) $Na_{12}A$ exchanged with $^{109}Ag^+$ shows only $Ag^0(A)$ which does not change on brief warming to $\sim$100 K.

observed. As shown in Figure 2, at intermediate exchange levels of Mg^{2+}, $Ag^0(C)$ is seen as the dominant species immediately after γ-irradiation but is converted to $Ag^0(A)$ on brief warming to $\sim$100 K. However, in Na_2Mg_5A, the zeolite with the highest level of magnesium exchange, $Ag^0(C)$, disappears on warming and is not converted to $Ag^0(A)$ (see Figure 2c,d) or any other ESR-detectable species. As shown in Figure 2e, $Ag^0(A)$ is not affected by warming $Na_{12}A$ to 100 K during which time the hydrogen atom and $Ag^0(B)$ species decay rapidly. It is interesting to note that $Ag^0(C)$ is not formed in Sr_6A, K_2Zn_5A, Cd_6A, or Ba_6A zeolites.

The principles of the formation of electron spin echoes and their modulation by nearby magnetic nuclei have been extensively discussed.[18,19] On application of resonant microwave pulses in suitable sequences to a spin system, microwave echoes are observed owing to re-formation of macroscopic magnetization. For a two-pulse sequence separated by time τ, the echo forms after a second time, τ after the second pulse. In a three-pulse sequence, the echo is obtained at $T + \tau$ after the second pulse, where T is the interval between the second and third pulses. On sweeping the time intervals, the echoes decay owing to various relaxation processes, and the echo decay envelope is obtained. The time-dependent magnetic field produced by the nearby magnetic nuclei at the site of the unpaired electron spin causes modulation of the echo decay envelopes at frequencies close to the Larmor precession frequencies of the magnetic nuclei. In analysis of such data, an electron-nuclear point dipole approximation is assumed.[18] In a powder sample, a spherical averaging approximation is used in which the nuclei responsible for the modulations are assumed to be randomly distributed over a sphere.[19] In principle it is possible to distinguish modulations from fixed geometries but such a distinction becomes meaningful for deuterons only when the electron-nuclear distances are less than 0.3 nm.[25] Simulations of the normalized echo modulations are made as a function of the average number of nearest interacting nuclei, n, at a distance r and with an isotropic hyperfine coupling a_{iso}. The normalized modulations are multiplied with a polynomial decay function, obtained empirically from the experimental data and compared with the experimental spectra. In the simulations n is constrained to integral values, and for $n < 10$, n can be determined to the

(23) Narayana, P. A.; Kevan, L. *Photochem. Photobiol.* **1983**, *37*, 105.
(24) Kevan, L.; Narayana, M. In "Intrazeolite Chemistry", ACS Symposium Series Stucky, G., Ed.; No. 218; American Chemical Society: Washington, D.C., 1983; p 283.
(25) (a) Kevan, L.; Bowman, M. K.; Narayana, P. A.; Boeckman, R. K.; Yudanov, V. F.; Tsvetkov, Yu.D. *J. Chem. Phys.* **1975**, *63*, 409. (b) Narayana, P. A.; Bowman, M. K.; Kevan, L.; Yudanov, V. F.; Tsvetkov, Yu. D. *Ibid.* **1975**, *63*, 3365.

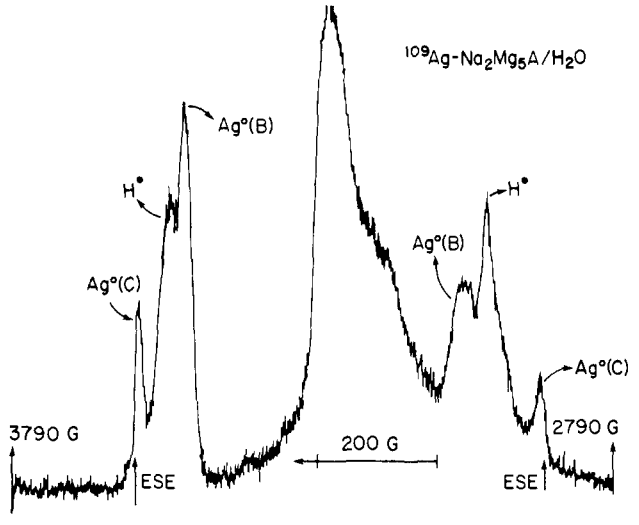

Figure 3. ESE-induced ESR spectrum at 4.2 K of Ag^0 in Na_2Mg_5A zeolite. The arrows marked ESE indicate magnetic field positions at which ESEM spectra were recorded. The arrows at each end of the spectrum indicate the magnetic field scale. The large center line at $g = 2$ is due to OH and zeolite radicals.

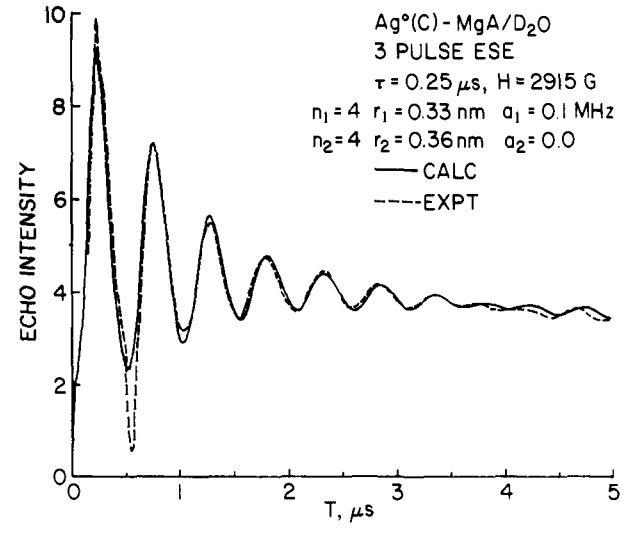

Figure 4. Calculated and experimental three-pulse ESEM spectra at the low-field $Ag^0(C)$ transition in Na_2Mg_5A exchanged with $^{109}Ag^+$. The best fit was obtained for a two-shell model and the decay function used in the calculation is $g(T) = \exp(2.33 - 0.07T + 0.008T^2)$. The line distortions seen in the experimental data near $\tau \sim 0.5$ μs are due to interference from two-pulse echoes.

nearest integer; r is typically determined to ±0.01 nm and a_{iso} to ±10%.

Figure 3 shows an ESE-induced ESR spectrum, obtained by scanning the magnetic field for a fixed interpulse time of 0.37 μs in a two-pulse echo sequence. Figures 4 and 5 show the experimental and calculated three-pulse ESEM spectra for deuterium modulations. The best fits for these and other three-pulse spectra were obtained with a two-shell model, four deuterons interacting with Ag^0 at 0.33 nm with an isotropic coupling of about 0.1 MHz and four other deuterons at 0.36 nm. Note that Figure 4 gives the data recorded on the low-field ESR line of $Ag^0(C)$ while Figure 5 gives the data recorded on the high-field ESR line of $Ag^0(C)$, and the agreement of the best fit parameters between these two sets of data is excellent.

In principle it is possible to analyze the ESEM data by fast Fourier transformation (FFT) of the time domain data into the frequency domain.[26] However, the quantitative aspects of these

(26) Blumberg, W. E.; Mims, W. B.; Zuckerman, D. *Rev. Sci. Instrum.* **1973**, *44*, 546.

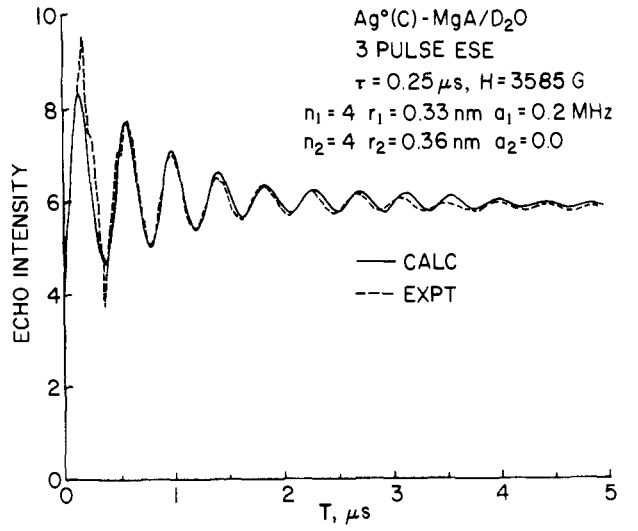

Figure 5. Calculated and experimental three-pulse ESEM spectra at the high-field $Ag^0(C)$ transition in Na_2Mg_5A exchanged with $^{109}Ag^+$. The decay function used in the calculation is $g(T) = \exp(2.15 - 0.015T)$. The best fit was obtained for a two-shell model and the parameters agree well with those in Figure 4. The line distortions seen in the experimental data near $\tau \sim 0.5$ μs are due to interference from two-pulse echoes.

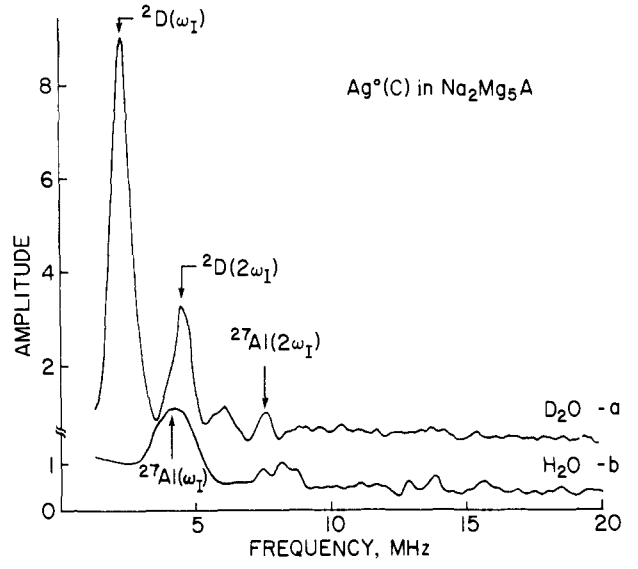

Figure 6. Fast Fourier transforms of experimental two-pulse ESEM spectra of $Ag^0(C)$ in (a) Na_2Mg_5A/D_2O and (b) Na_2Mg_5A/H_2O. The arrows indicate the expected free precession frequencies of ^{2}D and ^{27}Al nuclei at a magnetic field of 3585 G. See Table I.

Table I. Hyperfine Frequencies in Ag–MgA Zeolite

nucleus	Larmor frequency,[a] MHz	obsd frequency, MHz
^{1}H	15.33	15.54
^{2}D	2.34	2.28
	4.69[b]	4.55
^{27}Al	3.97	4.00, 4.3
	7.95[b]	7.72, 8.7
		6.14

[a] At 3585 G. [b] Second harmonic of the Larmor frequency.

frequency spectra are still in the process of development.[27,28] While the frequencies can be directly obtained from such a FFT spectrum, the intensities of the peaks are not reliable enough to

(27) Mercks, R. P. J.; DeBeer, R. *J. Magn. Reson.* **1980**, *37*, 305.
(28) (a) Aruna, B.; Ramakrishna, Y. V. S.; Narayana, P. A. *Phys. Status Solidi B* **1980**, *101*, 791. (b) Narayana, P. A.; Kevan, L. *J. Magn. Reson.* **1982**, *46*, 84. (c) Narayana, P. A.; Kevan, L. *Magn. Reson. Rev.* **1983**, *7*, 239.

give the number of nuclei at each frequency. Figure 6 shows such an FFT spectrum of the two-pulse ESEM spectra of the hydrated and deuterated samples of Ag-Na_2Mg_5A zeolites. It is found that the ^{27}Al frequencies are extremely sensitive to the extent of hydration of the zeolite as shown by Figure 6b in which Ag-Na_2Mg_5A was briefly evacuated at room temperature. The frequencies observed in samples obtained by dehydration and subsequent hydration (or deuteration) were highly reproducible These are tabulated in Table I.

Discussion

A brief description of the A zeolite structure[29] is useful to better understand the above-mentioned results. Alternating AlO_2 and SiO_2 bridges form a truncated octahedron called the sodalite or β-cage, and several of these sodalite cages are bridged on their square faces to form the cubic unit cell of A zeolite. The larger cage formed by the coupling of the sodalite cages is called the α-cage or super cage. Because of the excess negative charge on the AlO_2 units, charge-compensating cations are required to preserve charge neutrality. The primitive unit cell of the sodium form of A zeolite has a typical molecular formula of $Na_{12}Al_{12}Si_{12}O_{48}\cdot 27H_2O$ in which the sodium ions are the charge-compensating cations and are ion exchangeable with other mono- or divalent cations. These exchangeable cations are usually present at two specific sites, namely in the six-ring windows between the α- and β-cages (site S2) and in the eight-ring window entrances to the α-cage. Silver ions are known to have a high affinity for the six-ring window S2 sites in A zeolite.[30] No crystal structure data are available for highly magnesium-exchanged A zeolite, but in zeolites with different exchangeable divalent cations, Ca^{2+} and Sr^{2+} were shown[31-33] to have preference for the six-ring window sites as well. From ESEM analysis of $Ag^0(A)$ in several A zeolites, we have shown that this silver species is in the sodalite cages coordinating to two water molecules.

The smaller hyperfine coupling of $Ag^0(C)$ compared with that of $Ag^0(A)$, 1778 vs. 1980 MHz, indicates that the environments of these two types of isolated silver atoms are significantly different. As mentioned in the Results section, $Ag^0(C)$ is stable only below 100 K. It is interesting that the resulting product from its decay strongly depends on the type of exchangeable cation present in the zeolite structure. In sodium- or lithium-rich zeolites, loss of $Ag^0(C)$ always results in enhancement of $Ag^0(A)$. As seen in Figure 2 this is not the case when Mg^{2+} is the major cation. Since no other ESR detectable species were observed after the decay of $Ag^0(C)$ on brief warming, it is likely that either Ag^+ is formed by loss of an electron or a diamagnetic silver atom cluster is formed. From the charged clusters observed on decay of $Ag^0(A)$ in our earlier study,[20] the second possibility is more likely.

It is important to note that the formation and enhancement in the intensity of $Ag^0(C)$ is very strongly dependent upon the presence of Mg^{2+} in the zeolite. Since $Ag^0(C)$ is not observed in Sr_6A, K_2Zn_5A, Cd_6A, or Ba_6A and is only observed as a weak species in Ca_6A, it is clear that the presence of divalent cations alone is not sufficient for formation of $Ag^0(C)$. Since the magnesium-exchanged zeolites have more water molecules per unit cell than the others (e.g., $Na_{12}A$ has 27, Ca_6A has 31) we tried 77 K γ-irradiation of aqueous suspensions of silver-exchanged $Na_{12}A$ but were unable to form $Ag^0(C)$. As shown in Figure 1b, very small quantities of Mg^{2+} in the zeolite were sufficient to induce the formation of $Ag^0(C)$, and its intensity increased substantially at the cost of $Ag^0(A)$ on increasing the Mg^{2+} content in the unit cell (see Figure 2a).

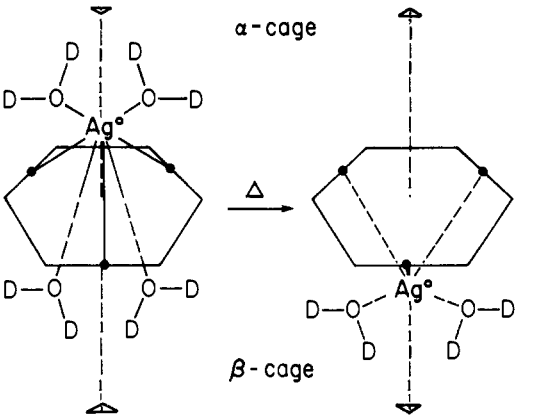

Figure 7. Possible location of $Ag^0(C)$ in A zeolite. $Ag^0(C)$ is placed slightly above the center of the six-ring window, projecting into the α-cage at site S2*. The dotted normal to the six-ring window is the threefold axis. In A zeolites with Na $\geq$ 8 and Mg $\leq$ 2, it is suggested that on warming the $Ag^0(C)$ moves along the threefold axis to an S2′ site in the β-cage to form $Ag^0(A)$.

Analysis of the ESEM data shown in Figures 4 and 5 indicate that $Ag^0(C)$ interacts with four deuterons at 0.33 nm with a small hyperfine coupling of 0.1 to 0.2 MHz and four more deuterons at 0.36 nm. These eight deuterons could be interpreted as coming from two closer water molecules and two further ones. If we assume the dipole of the D_2O molecule is along the Ag–O_w bond and pointed away from Ag, then the closer deuterons indicate an Ag–O_w distance of 0.26 nm which is consistent with Ag–O distances observed in several crystallographic studies[30] of Ag^+-exchanged A zeolites. The farther waters indicate an Ag–O_w distance of 0.29 nm; since this is larger than the sum of Ag^+ and O^{2-} radii, these waters are less weakly coordinated to the silver atom. From ESEM studies of silver atoms in ice matrices, Narayana et al.[14a] and Ichikawa et al.[14b] have shown that a presolvated silver atom interacts with four equivalent water molecules in a tetrahedral configuration. The hyperfine coupling of such a presolvated silver atom, 1760 MHz, is slightly less than that of $Ag^0(C)$, 1778 MHz, which could be interpreted as a small difference in the solvation geometry of the silver atom. $Ag^0(C)$ could thus be a silver atom in the α-cage interacting with four water molecules in the α-cage in a very distorted tetrahedral configuration.

Since the α-cage diameter is 1.1 nm, such an $Ag^0(H_2O)_4$ complex can be accommodated very easily. However, if $Ag^0(C)$ is at the center of the α-cage, it would be far from the framework Al^{3+} (>0.5 nm), and very little or no aluminum modulation would be expected in the ESEM spectra. The aluminum modulation we observe for $Ag^0(C)$ could not be quantitatively analyzed because of complications by nuclear quadrupole interactions, but they seem indicative of an Ag–Al distance less than 0.43 nm. Furthermore, in sodium-rich zeolites the conversion of $Ag^0(C)$ to $Ag^0(A)$ indicates that these two sites are not too far from each other. We have already shown[20] that $Ag^0(A)$ is in the β-cages at S2′ sites, which are displaced from the S2 sites in the center of the six-ring window into the β-cages along the threefold axis perpendicular to the six-ring window. It is well established from many crystallographic studies[30] that Ag^+ ions occupy the S2 sites. Thus it is unlikely that they will move very far from this site after electron capture at 77 K.

The following model is suggested to explain the two inequivalent shells of interacting waters of $Ag^0(C)$ and the conversion of $Ag^0(C)$ to $Ag^0(A)$. If Ag^+ at S2 sites moves upon electron capture along the threefold axis perpendicular to the six-ring window into the α-cage, this is designated as site S2* and any water molecules inside the β-cage coordinated to the newly formed $Ag^0(C)$ would be farther from $Ag^0(C)$ than any coordinated water molecules in the α-cage. As shown in Figure 7 then, the two closer water molecules to $Ag^0(C)$ can be assigned to be in the α-cage and the two farther waters to be inside the β-cage. On warming the samples, $Ag^0(C)$ moves along the threefold axis from the S2*

(29) Barrer, R. M. "Zeolites and Clay Minerals"; Academic Press: London, 1978; p 76.
(30) (a) Kim, Y.; Seff, K. *J. Am. Chem. Soc.* **1977**, *99*, 7055. (b) Kim, Y.; Seff, K. *J. Phys. Chem.* **1978**, *82*, 1307. (c) Gellens, L. R.; Smith, J. V.; Pluth, J. J. *J. Am. Chem. Soc.* **1983**, *105*, 57.
(31) (a) Firov, R. L.; Seff, K. *J. Am. Chem. Soc.* **1977**, *99*, 7059. (b) McCusker, L. B.; Seff, K. *Ibid.* **1978**, *100*, 5052.
(32) Pluth, J. J.; Smith, J. V. *J. Am. Chem. Soc.* **1982**, *104*, 6977.
(33) Schollner, R.; Gellens, L. R.; Mortier, W. J.; Uytterhoeven, J. B. *Zeolites* **1983**, *3*, 149.

position in the α-cage to the S2′ position inside the β-cage where it interacts with only two waters and becomes $Ag^0(A)$. This model accounts for the inequivalence of the water molecules around $Ag^0(C)$ and conversion of $Ag^0(C)$ to $Ag^0(A)$ in sodium-rich zeolites.

While the location of $Ag^0(C)$ in Mg^{2+}-rich zeolites is also probably at site S2* in the α-cage, the decay product of $Ag^0(C)$ is unclear. It should be noted that the possibility of $Ag^0(C)$ being inside the β-cages seems ruled out by comparison of its thermal instability with $Ag^0(D)$ observed in X and Y zeolites which has been shown[20] to be thermally stable and to interact with four *equivalent* water molecules inside the β-cage.

In the photochemical water cleavage experiments,[10a] zeolites exchanged with Mg^{2+} were found to be most efficient. Isolated or small clusters of silver atoms have been implicated in the water splitting. Since $Ag^0(C)$ is enhanced by Mg^{2+}, we suggest that it could be the active intermediate in such a reaction.

Conclusions

The minor species $Ag^0(C)$ observed earlier in $Li_{12}A$ and Ca_6A zeolites becomes a major Ag^0 species by ion exchange of A zeolite with Mg^{2+} prior to doping by Ag^+. In A zeolites containing Mg^{2+} but still richer in sodium, $Ag^0(C)$ decays to $Ag^0(A)$ on warming above 100 K. In fully sodium-exchanged A zeolite only $Ag^0(A)$ is seen. ESEM analysis indicates that $Ag^0(C)$ interacts with two water molecules at an Ag^0–O_w distance of 0.26 nm, which are suggested to be in the α-cage, and with two more water molecules at an Ag^0–O_w distance of 0.29 nm, which are suggested to be in the β-cage. We suggest that $Ag^0(C)$ is located at site S2* in the α-cage just above the six-ring window between the α- and β-cages and moves to S2′ sites in the β-cage below the six-ring window to form $Ag^0(A)$ when the zeolite contains sufficient numbers of Na^+ ions.

Acknowledgment. This research was supported by the National Science Foundation and the Robert A. Welch Foundation. We thank the Energy Laboratory of the University of Houston for equipment support, Mr. Randy Wilkin for his help in sample preparations, and Dr. Sal Contarini for the thermogravimetric measurements.

Registry No. Ag, 7440-22-4; Mg, 7439-95-4; Na, 7440-23-5.

Electrochemistry, Spectroelectrochemistry, and Photochemistry of a Series of New Covalently Linked Tris(2,2′-bipyridine)ruthenium(II)/Diquat Complexes

C. Michael Elliott,* Ruth A. Freitag,† and David D. Blaney

Contribution from the Department of Chemistry, Colorado State University, Fort Collins, Colorado 80523. *Received December 17, 1984*

Abstract: A method for preparing covalently linked photosensitizer/electron-acceptor complexes using a novel dimer of 4,4′-dimethyl-2,2′-bipyridine has been found. N,N′-Dialkylation of one end of the dimer results in a "diquat"-modified ligand which can be bound to Ru(II) in combination with other substituted or unsubstituted bipyridines. A series of tris(bipyridine)ruthenium/diquat complexes was prepared in which the properties of both the diquat electron acceptor and the ruthenium photosensitizer were varied. The effect of the detailed structure of these linked systems on their electrochemical, spectroelectrochemical, and photophysical properties was investigated.

Photoinduced bimolecular electron-transfer reactions involving a tris(bipyridine)ruthenium photosensitizer and an electron acceptor such as the dipyridinium salt paraquat have been extensively investigated.[1-4] A few examples of similar unimolecular systems have also been reported.[5-7]

In order to examine the relationships between the detailed structures of both the photosensitizing moiety and electron acceptor, and the photochemical and electrochemical properties of the system, a series of linked tris(bipyridine)ruthenium/electron-acceptor complexes has been prepared. The synthetic method by which an inert, covalent linkage between photosensitizer and acceptor has been accomplished is based on a novel dimer of 4,4′-dimethyl-2,2′-bipyridine, Mebpy–Mebpy, **1**, Conversion of one of the linked bipyridines of **1** to an N,N′-bridged diquaternary salt (diquat) produces an electron acceptor with properties similar to those of paraquat.[4] This conversion yields the ligands Me-bpy–*n*DQ^{2+}, where *n* is the number of methylene units in the chain linking the pyridine nitrogens (**2**, $n = 2$; **3**, $n = 3$).

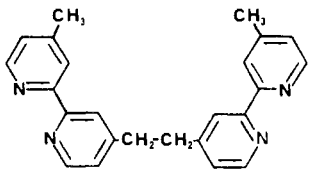

1

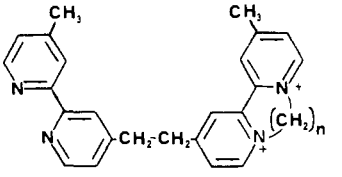

2, n=2
3, n=3

† Present address: Department of Chemistry, Davidson College, Davidson, NC 28036.

(1) Whitten, D. G. *Acc. Chem. Res.* **1980**, *13*, 83.
(2) Sedden, K. R. *Coord. Chem. Rev.* **1982**, *41*, 137.
(3) Zamaraev, K. I.; Parmon V. N. *Russ. Chem. Rev.* (*Engl. Transl.*) **1983**, *52*, 817.
(4) Kalyanasundaram, K. *Coord. Chem. Rev.* **1982**, *46*, 159.
(5) Westmoreland, T. D.; Le Bozec, H.; Murray, R. W.; Meyer, T. J. *J. Am. Chem. Soc.* **1983**, *105*, 5952.
(6) Matsuo, T.; Sakamoto, T.; Takuma, K.; Sakura, K.; Ohsako, T. *J. Phys. Chem.* **1981**, *85*, 1277.
(7) Elliott, C. M.; Freitag, R. A. *J. Chem. Soc., Chem. Commun.* **1985**, 156.

0002-7863/85/1507-4647$01.50/0